J. Mt. Sci. (2011) 8: 641–654
DOI: 10.1007/s11629-011-1030-1

Fractal Measures of Drainage Network to Investigate Surface Deformation from Remote Sensing Data: A Paradigm from Hindukush (NE-Afghanistan)

Syed Amer MAHMOOD[1,2] * **Richard GLOAGUEN**[1]

1 Remote Sensing Group, Institute of Geology, Freiberg University of Mining and Technology, Freiberg, 09599, Germany

2 Department of Space Science, University of the Punjab, New Campus, 54590, Lahore, Pakistan

**Corresponding author, e-mail: amerpakistan@gmail.com*

Abstract: This approach represents the relative susceptibility of the topography of the earth to active deformation by means of geometrical distinctiveness of the river networks. This investigation employs the fractal analysis of drainage system extracted from ASTER Global Digital Elevation Model (GDEM-30m resolution). The objective is to mark active structures and to pinpoint the areas robustly influenced by neotectonics. This approach was examined in the Hindukush, NE-Afghanistan. This region is frequently affected by deadly earthquakes and the modern fault activities and deformation are driven by the collision between the northward-moving Indian subcontinent and Eurasia. This attempt is based on the fact that drainage system is strained to linearize due to neotectonic deformation. Hence, the low fractal dimensions of the Kabul, Panjsher, Laghman, Andarab, Alingar and Kocha Rivers are credited to active tectonics. A comprehensive textural examination is conducted to probe the linearization, heterogeneity and connectivity of the drainage patterns. The aspects for these natural textures are computed by using the fractal dimension (FD), lacunarity (LA) and succolarity (SA) approach. All these methods are naturally interrelated, i.e. objects with similar FD can be further differentiated with LA and/or SA analysis. The maps of FD, LA and SA values are generated by using a sliding window of 50 arc seconds by 50 arc seconds (50" × 50"). Afterwards, the maps are interpreted in terms of regional susceptibility to neotectonics. This method is useful to pinpoint numerous zones where the drainage system is highly controlled by Hindukush active structures. In the North-Northeast of the Kabul block, we recognized active tectonic blocks. The region comprising, Kabul, Panjsher, Andrab, Alingar and Badakhshan is more susceptible to damaging events. This investigation concludes that the fractal analysis of the river networks is a bonus tool to localize areas vulnerable to deadly incidents influencing the Earth's topography and consequently intimidate human lives.

Keywords: Fractal; Drainage network; Lacunarity; Succolarity; Surface deformation and Hindukush

Received: 12 April 2010
Accepted: 10 January 2011

Introduction

The fractal geometry has received increased attention as a novel model for natural phenomena. Composite branching architecture and dendritic shape of drainage network make the impression of fractal-like structure. Superimposition of diverse physical and geological processes governing the development of rivers, including also random components, produces fractal river networks (Dombradi et al. 2007). Computation of spatial patterns and their detailed analysis using nonlinear approach is growing in tectonic geomorphology, landscape ecology, information sciences, forestry, life sciences, food research and peripheric systems (Dong 2009; Valous et al. 2009; Mahmood et al. 2009; Shahzad et al. 2010; Dombradi et al. 2007; Gloaguen et al. 2007; Martinez et al. 2007; Feagin et al. 2007; Ting et al. 2006; Buston et al. 2006; Melo et al. 2006; Dougherty and Henebry 2002). The prime objective of these methodologies is to spot the diversities in natural patterns and study their causes. In morphotectonic investigation, these diversities appear in the form of breaks, linearity and irregularities in drainage network due to the ongoing exterior and interior geological processes. The three FD (fractal dimension) measures are complimentary and periodic in nature, that is if two sets could have the same FD and be differentiated by Lacunarity analysis (LA), On the same way, the notions of Succolarity analysis (SA) makes possible to distinguish

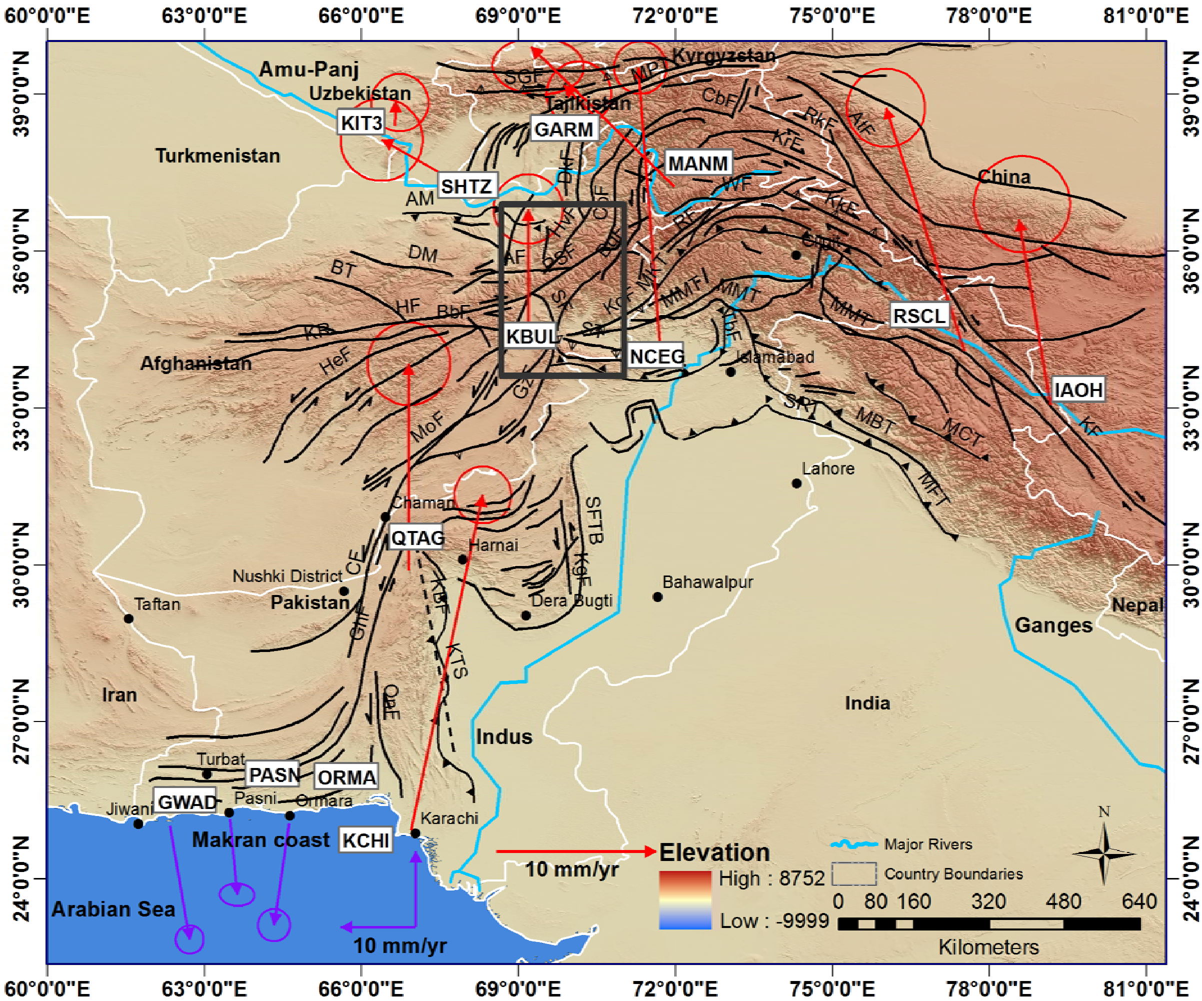

Figure 1 Structual map of the Hindukush-Himalaya-Pamir-Karakoram showing reported and newly confirmed faults with inset showing the study area (Figure 2). GPS velocity vectors (Red) with respect to Eurasia fixed reference frame from (Mohajder et al. 2010), the purple vector is transformed from (Khan et al. 2008) wit respect to India fixed. Abbreviations of fault names: DkF, Darvaz Karakul Fault, AM, Alburz Marmul, CbF, Central Badakhshan Fault, HvF, Henjvan fault, HF, Herat Fault, CF, Chaman Fault; MoF, Mokar fault, GzF, Gardez Fault, KoF, Konar Fault, SBF, Sulaiman Base front, MBT, Main Boundary Thrust; MFT, Main frontal thrust, MMT, Main Mantle Thrust, and MKT, Main Karakoram Thrust, Reshun Fault, TMF, Tirch Mir Fault, SF, Sarobi Fault, ST, Spinghar Thrust, AF, Andarab Fault, TbF, Tarbella Fault, BgF, Bazgir Fault (after Lawrence et al. 1981; Bannert et al. 1992; Searle and Khan 1996; Wheeler et al. 2005; Ruleman et al. 2005; Doebrich and Wahl 2006).

different sets or textures that have the same FD and LA or vice-versa and the drainage patterns can record their cumulative effects (Mahmood et al. 2008; Mahmood et al. 2009; Bull 2007). Preceding appraisals have anticipated that the linear (Brookfield et al. 2008; Wobus et al. 2006; Mahmood et al. 2009) and nonlinear analysis (Dombradi et al. 2007; Gloaguen et al. 2007; Mahmood et al. 2009; Shahzad et al. 2010) of individual streams as well as the whole drainage system may be analyzed to examine the surface deformation. The linear analyses chiefly focus on the secondary parameters (contributing drainage area, channel lengths, channel slope, elevation and etc.), and completely overlook the fractal behaviour of drainage network. A typical linear approach e.g. stream profile analysis (Wobus et al. 2006; Mahmood et. al. 2008; Shahzad et al. 2009) uses the slope-area correlation which generate same results for dissimilar causative effects. These effects can be abridged if the spatial distribution of the drainage system is taken into consideration.

Fractal measures (FM) is a powerful tool as patterns with dissimilar space filling characteristics can easily distinguish those areas, which yield same signatures using the conventional linear analysis. The space filling style of the drainage network is a sturdy marker of the area susceptible to surface deformation. The drainage network adapts them to reorganize and linearize (Gloaguen et al. 2008; Mahmood et al. 2009; Shahzad et al. 2010). Consequently we use nonlinear analysis (fractal measures) i.e. FD, LA and SA to epitomize the irregularity of drainage network and to compute the transformation from a dendritic pattern into a tectonically controlled one. These analyses permit the investigation of textural characteristics of the drainage network and are strongly helpful to assess the demarcation and intensity of surface deformation. The FM was applied to the drainage systems of the western Hindukush and its outskirts (Figure 1). The drainage pattern in the region is the result of spatially inconsistent tectonic and erosional processes (Mahmood et al. 2008) and shows region with erratic susceptibility to surface deformation (Ruleman et al. 2005, Mahmood et al. 2008). In a high seismic framework, the anomalous, incoherent and linearized drainage patterns give inspiration for this research.

The drainage network was extracted from ASTER Global Digital Elevation Model (ASTER GDEM-30m resolution) using D8 algorithm (Jenson and Domingue 1988). The Box Counting method (Gloaguen et al. 2007; Dombradi et al. 2007) calculated the fractal dimension (FD) of the Kabul, Panjsher, Laghman, Andarab, Alingar and Kocha rivers to recognize their inconsistent drainage behavior. The FD distribution map was generated based on the analyzed drainage network. The LA and SA were tested for 10 sample sites having the same FD to assess their behaviour and these regions exhibit similar translational invariance to some extent. However, regions with similar FD values signify very diverse drainage textures, which need further differentiation. The gliding box method (Melo et al. 2006; Dombradi et al. 2007) was employed for the LA (Λ) to prepare lacunarity map. The SA (σ) was used to compute the gyration regularity of the drainage network and to examine the gyration of the drainage pattern with the same translation behavior. The SA computes the percolation capacity of the underlying binary image (Shahzad et al. 2010; Melo and Conci 2008) of the spatial drainage pattern in the horizontal (left to right, L2R and right to left, R2L) as well as vertical directions (top to bottom, T2B and bottom to top, B2T) . We generated the SA map in the same way as we did for FD and LA. For the 10 selected regions, mean SA value was used to distinguish the comparative diversity where the drainage network exhibits same translation invariance and is unidentified by LA and FD. The FD, LA and SA (Distribution, translation invariance and rotation) of drainage network are interrelated directly connected with the active tectonic deformation. The FD yields the distribution of drainage network low FD values like 1 means a region of an extreme surface deformation. The translation invariance is given by LA and a low value of lacunarity means less surface deformation. The SA characterizes the style of orientation of the drainage network influenced by the general patterns and the orientations of the tectonic units and higher mean SA values are an indication of extremely deformed regions.

1 Study Area

Non-linear analysis and digital mapping of the tectonically deformed Hindukush using remote sensing data is of crucial significance in the context of tectonic geomorphology, geology, seismic hazard assessment and human protection. The study area comprises some of the major settlements in NE-Afghanistan including the capital city Kabul, Jalalabad, Panjsher valley, Qunduz, Alingar, Badakhshan and Khanabad (Figure 2).

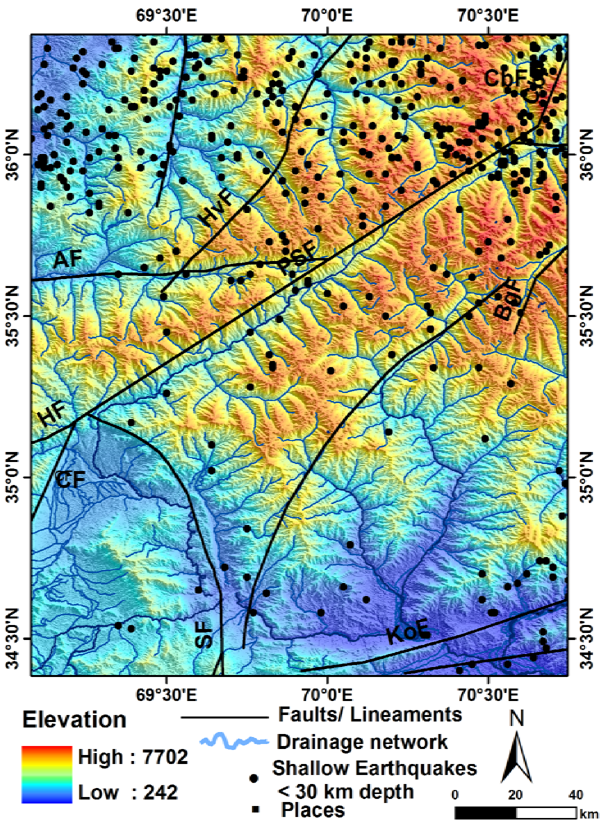

Figure 2 Tectonic map of the study area in Afghanistan. Showing regional faults, drainage network and shallow (< 35 km deep) historical earthquakes (Dewey 2006) in Hindukush.

As neotectonic deformation continues in this region, moderate-to-large magnitude, potentially destructive earthquakes are frequent and will continue to occur, these earthquakes will possibly cause stern damage, not only from strong ground shaking and faults rupturing the ground surface, but also from liquefaction and extensive landsliding, as occurred during the devastating October 8, 2005, M 7.6 Kashmir earthquake in nearby northern Pakistan (Harp and Crone, 2006). The variety of destructive and deadly hazards associated with earthquakes poses a real and serious threat to reconstruction efforts and to the economic growth and development of this region. Consequently, it is extremely vital to localize the regions prone to surface deformation and to examine the seismic hazard assessment. Hindukush-Afghanistan is situated in central Asia in the tectonically active Alpine-Himalayan orogenic belt that developed due to the ongoing collision between the Indian, Arabian and Eurasian plates in Late Paleogene to Recent (65 million years ago to the present) time (Harp and Crone, 2006). As the Eurasian continent was being assembled prior to 65 million years ago, numerous episodes of deformation had already shattered and buckled the crust in and around Afghanistan. The study area is located NNE of the Kabul block, we observed a complex pattern of potentially active strike-slip and thrust faults based on their geomorphic expression. The major rivers draining the study area are the Kabul, Panjsher, Laghman, Andarab, Alingar and Kocha. The major tectonic features in this region are Andarab Fault (AF), Chaman Fault (CF), Central Badakhshan (CB), Darvaz Fault (DF), Gardez (GF), Heart Fault (HF), Henjvan Fault (HF), Konar Fault (KF), Paghman Fault (PF), Panjsher Fault (PSF), Sarobi Fault (SF), and Spinghar Fault (SPF). The study area exhibits variable style of deformation which provides an insight into the kinematics of the recent tectonism, and describe a tectonic framework that can help to constrain deformational models of the Alpine-Himalayan orogenic belt. NW-trending strike-slip faults are cut and displaced by younger, SE-verging thrust faults, these relations describe the interaction between NW-SE-oriented contraction and NW-directed extrusion in the Hindukush-Pamir and western Himalayan regions (Allen et al. 2004, Ruleman 2005, Wheeler et al. 2005).

2 Computing Methodologies

The drainage network was extracted from ASTER Global Digital Elevation Model (GDEM-30m resolution) and a binary image was prepared. Before the drainage network extraction, the pits/holes/depressions were removed from the data by DEM processing. The D8 flow grid algorithm (Jenson and Domingue 1988, O'Callaghan and Mark 1984) computes the potential flow guidelines at every pixel towards the bordering 8 pixels. The least cost path algorithm is used to fix a constant drainage network. The extracted drainage is then filtered to represent the streams with a contributing area > 1 km² so as to keep only those parts where efficient flow occurs to avoid hill slope diffusion (Tarboton et al. 1991). We used the streams of Strahler order higher than or equal to 6 in order to diminish the noise in the DEM. Finally, binary image of the drainage network was prepared where the streams have a pixel value of 1 and rest of the space is treated as zero (Melo et al. 2006, Melo at el. 2008, Plotnick et al. 1996, Plotnick et al. 1993). In the current investigation, we anticipate that the drainage network becomes linearized as the study area is strongly controlled by neotectonics. The FD technique is vague, because it simply indicates the amount of the network complication, and does not demonstrate the pattern depiction. This is why the LA and SA (Mandelbrot, 1983) approaches are employed to portray the pattern recognition. These techniques have been explained with the help of a simplified flow algorithm chart as shown in Figure 3.

2.1 Fractality: geometrical distribution and complexity

Several studies reveal that classical morphometric analysis poorly describes the complex natural features such as the drainage network of rivers. The drainage network displays irregularities with self-similar characteristics. The FD is a competent tool to quantify and describe geomorphological features and its usage has increased rapidly in the last 15–25 years (Gloaguen et al. 2007, 2008, Mandelbrot, 1983, Guillermo et al. 2004, Dombradi et al. 2007). The FD quantifies the degree of irregularity or fragmentation of an object of spatial pattern (Moreira 1999). In this investigation, the FD for the 6 selected rivers and the whole drainage network (Dombradi et al. 2007) is calculated using a box counting method (BCM). The BCM uses a moving box of variable size on an image and counts the number of drainage pixels within the box (Batty and Longley 1994, Foroutan-pour et al. 1999, Dombradi et al. 2007, Guillermo et al. 2004). In each grid, the box sizes S and relevant number of boxes $N(s)$ are counted. The FD

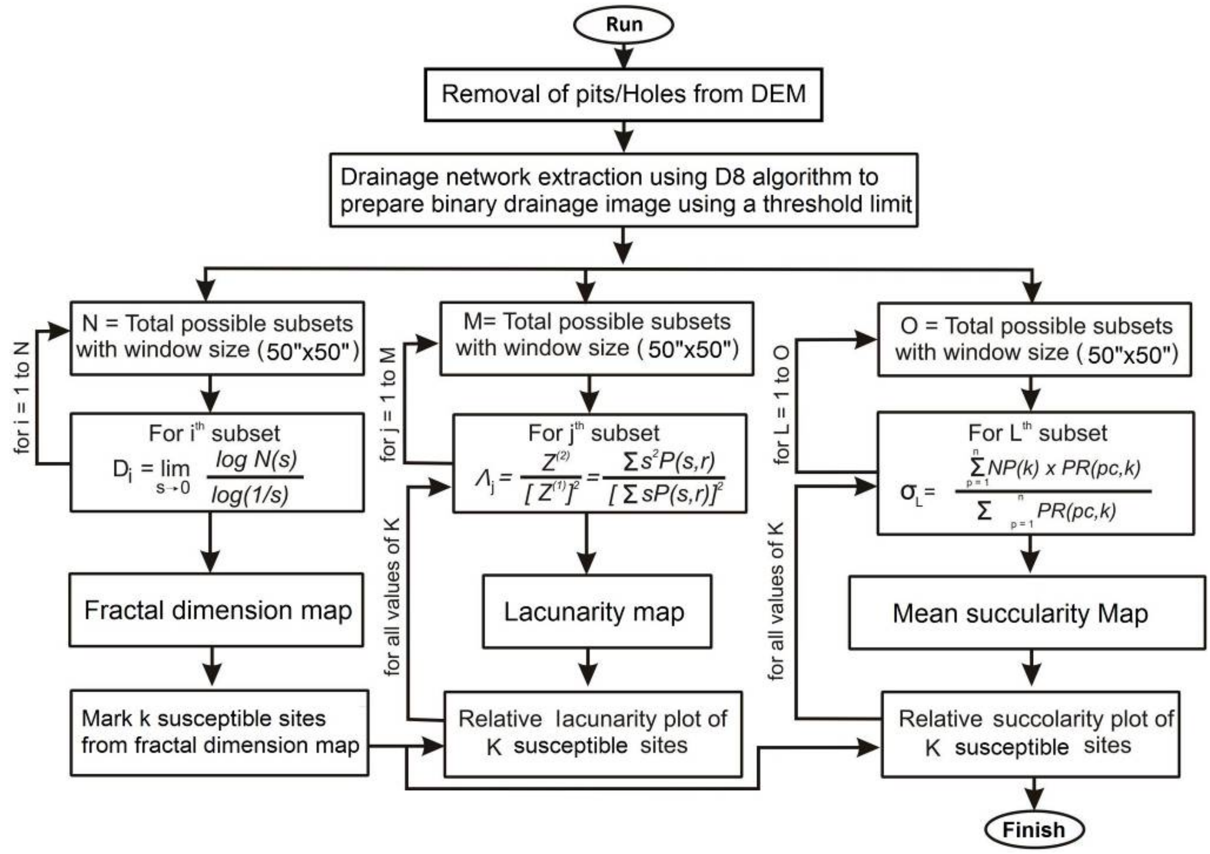

Figure 3 Flow charts showing various image processing steps (modified after Shahzad et al. 2010)

value is calculated by using the following equation.

$$FD = \lim_{s \to 0} \frac{\log N(s)}{\log(1/s)} \quad (1)$$

where *N(s)* is the number of boxes *and S* is the length of the box side applied. The slope of the best fit line for the log-log plot of *N(s)* and 1/s is equal to D. The BCM is used to compute the FD value of six regional rivers. A grid based approach was applied to examine the spatial distribution of FD, so as to evaluate the surface deformation processes. A moving window of 50 arc seconds by 50 arc seconds (50" × 50") on the binary image of the drainage network was used to calculate FD values for each window using Eq. (1). The FD distribution map was generated with color ramp so that the regions with smaller FD values can be recognized. Generally, The FD distribution map characterizes picture of the linearity of the drainage network. The low FD (when D→1), is related to highly linearized drainage patterns (Dombradi et al. 2007, Gloaguen et al. 2008) and hence shows the high susceptibility to surface deformation. The relative analysis of the spatial distribution of FD can be categorized in to three classes. The FD values less than 1.3 are allied with regions of high susceptibility to surface deformation, whereas the values > 1.3 and < 1.5 corresponds to medium susceptibility. The FD values > 1.4 correspond to the regions that are almost invariant.

2.2 Lacunarity: deviation from translational invariance

The LA measures the deviation of a fractal object from translational invariance. The LA can be used to better understand the textural depiction of the drainage patterns by studying the spatial distribution and sizes of vacant gaps (Plotnick et al. 1996; Dong 2000). The LA is a powerful tool to distinguish between the dissimilar textural patterns with similar FD values. The lacunarity of binary images can be calculated by different methods (Dong 2000; Melo et al. 2006), for instance, "Gliding Box method (GBM), Differential Box Counting", " three-term local quadrant variance" (3TLQV). We preferred to use the GBM for its simplicity, where a square box of side *r* is glided along all feasible direction of the drainage texture. The total number of drainage pixels (i.e. mass "s") is calculated during this whole gliding process. The GBM is repeated with sliding boxes of steadily growing size i.e. *r+i*. According to Plotnick et al. (1993), the gliding box should be of size *r* =1 to some fraction of image length (M). Consequently, a frequency distribution of mass "s" with variable box size r is obtained. This frequency distribution is transformed into a probability distribution P(*s,r*) by normalizing with the number of total boxes N(r) of size *r*. The dimensionless lacunarity Λ(*r*) is computed by the first and second moments of this distribution, as shown in the following equations (Plotnick et al. 1996, 1993).

$$\Lambda(r) = \frac{\sum_{r=1}^{N} s^2 P(s,r)}{\left[\sum_{r=1}^{N} sP(s,r)\right]^2} \quad (2)$$

The LA distribution map with a moving window of 50 arc seconds by 50 arc seconds (50″ ×50″) is prepared on the binary image of the drainage network. In all moving windows, the underlying image of 50″×50″ was taken as sub image and the box size of *r* =1 to 25 (< half of the moving window length as suggested by Plotnick et al. (1993)) was used to compute the lacunarity values. This procedure provides us with a distribution of box sizes vs. lacunarity values. We need a single lacunarity value which can be used as demonstration of the underlying area instead of the whole distribution and this single value of lacunarity should be carefully selected. Because, it can be observed on the log-log plots (Figure 4d), it changes with the resolution of the data set, i.e. high values of box sizes (e.g. *r* = 20, 25) will give low lacunarity and low values of r (e.g. 1, 2, 3) will give high values of lacunarity (Plotnick et al. 1993). To overcome the less mean error, we selected a middle value of box size at log(r) =1 and a matching value of lacunarity was obtained. This value can change from case to case depending upon data resolution and moving window size. We obtained a single lacunarity value at each pixel position. A spatial distribution of LA values was obtained by repeating this method for all moving windows. This LA distribution map of the study area is shown in Figure 4b. This method was also tested for all the sub regions of interest (ROIs) where similar FD values were found in Figure 4a. A composite plot of the LA values of all the10 identified ROIs was prepared. This plot was used to spot the relative susceptibility of the ROIs using high and low lacunarity values. A fractal object is translationally invariant if different parts of the object are similar. The LA value is associated to the distribution of gap sizes in a fractal object: homogeneous fractal objects have low LA values because all gap sizes are the same or almost the same, whereas heterogeneous fractals have high LA values because gap sizes are quite different. The drainage textures can exhibit translational invariance of the systems and can have high LA values accordingly. The high LA value is accredited to the heterogeneous drainage patterns i.e. highly deformed regions and vice versa. While doing the relative analysis, low LA values correspond to the low neotectonic activity (stable regions). The LA spatial distribution map can be divided into three categories i.e. low, medium and high lacunarity values. The values of $\Lambda(r)$ less than 1.5 characterize homogeneous drainage patterns and are connected with regions of low susceptibility of surface deformation. The $\Lambda(r)$ values from 1.5 to 2.5 stand for medium susceptibility and values higher than 2.5 correspond to heterogeneous drainage patterns and are related to highly deformed regions.

2.3 Succolarity: percolation and orientation

Succolarity (SA) is a natural evolution of the other well known fractal measures, i.e. FD and LA. The SA is an important feature in the pattern recognition process mainly for identification of natural textures. The SA measures the percolation degree of an image (draining capacity of an image), i.e., how much a given fluid can flow though this image (Mandelbrot 1983; Melo and Conci 2008).

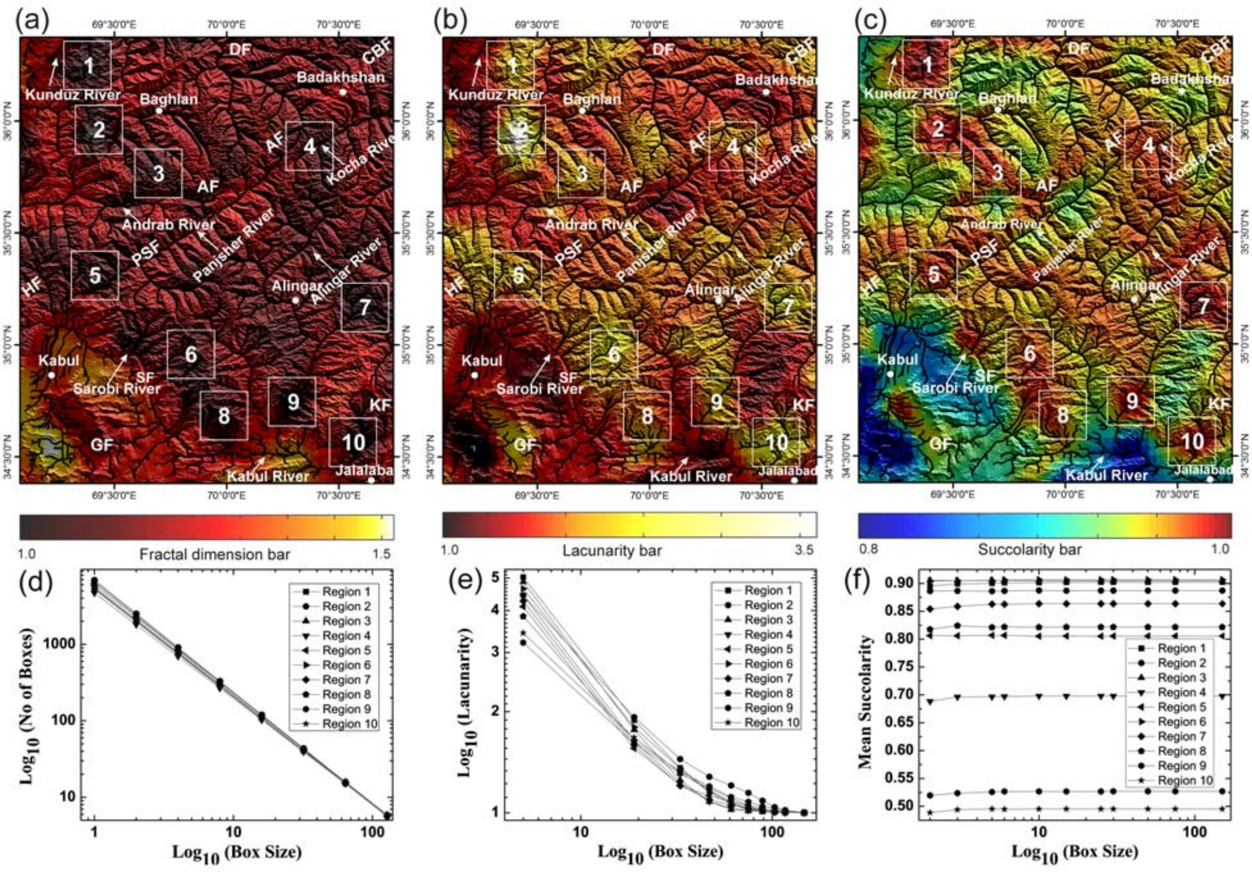

Figure 4 (a) FD distribution map of the study area. The low values of FD correspond to highly deformed areas. Ten sites with low values of FD are marked in the map. (b) LA distribution map of the study area where high LA values stand for the regions with high susceptibility of surface deformation. (c) SA distribution map with high values highlighting the severely deformed regions with low drainage density. The low values of SA indicate less deformed regions with high drainage density. (d), (e) and (f) Illustrate Fractal dimension, lacunarity and succolarity curves of the selected 10 sites were used to distinguish the relative vulnerability of surface deformation.

The SA becomes a proficient tool when the input texture has both direction as well as flow information associated with it e.g. drainage patterns. In the context of surface deformation, the SA measures the orientation of the geological structures. Succolarating fractals include the strings which allow percolation, i.e., the amount of interrelated pixels in drainage textures (Shahzad et al. 2010). These textures comprise two types of pixels, i.e. vacant gaps and impassable mass i.e. drainage. The SA was first introduced by (Melo and Conci 2008) using BCM. The SA can be measured along any possible flow direction (0°~360°). In order to measure the mean SA of the drainage pattern, we focused four likely directions, i.e. along 0°, 90°, 180° and 270°. The rotation image is prepared at the desired angle and the succolarity is calculated using the following four steps.

1) The binary image is inundated by checking all the boundary pixels coming from the top to bottom (T2B). If the pixel represents vacant gaps on the image (in our case we consider white as the absence in the pixel position), it means that a fluid can pass and flood this area. The existing material pixels (impenetrable mass-black drainage lines) are considered as obstacles to the fluid. All the flood areas from a boundary have their neighbors (4 neighbors for each pixel: Top, Bottom, Left and Right). This process is recursively executed on all the image pixels until the fluid encounters the material pixels (impenetrable mass).

2) The next step is then to analyze flooded area of each image using box counting approach like the BCM for FD calculation. In this approach, we place boxes of variable size *k* (*k*=1 to n), where n is the number of possible factor of divisions (Shahzad et al. 2010; Melo and Conci 2008) on the inundated image and then counting the number of flooding pixels (NP(k)) within the box.

3) For each box size, k, then the sum of the multiplications of the NP(k) by the pressure matrix PR(pc, k), where (pc is the position on x or y of the centroid of the box on the scale of pressure) applied to the box are calculated. The pressure matrix varies with the box size because it is applied on the centroid of the box. It also depends on the position of the box to correctly indicate the amount of pressure over it. The PR (pc, k) consists of linearly growing weight from T2B.

4) To make the SA value dimensionless like FD and LA we divide the value, NP(k) × PR(pc, k) by PR(pc, k), but now considering that the image was totally flooded by the fluid (as if the input image were totally black). The calculation is indicated in (3).

$$\sigma(dir) = \frac{\sum_{k=1}^{n} NP(k).PR(pc,k)}{\sum_{k=1}^{n} PR(pc.k)} \quad (3)$$

The (dir) represents the required flood/percolation direction of interest. The results of σ can be analyzed in many ways, i.e., along all direction or using the mean value. In case of huge data for comparison, we prefer to use the mean value to discern their draining characteristics. The mean SA value can be computed using the arithmetic mean of succolarity along four possible directions (T2B, B2T, L2R and R2L) suggested by (Melo and Conci 2008).

$$\overline{\sigma} = \frac{\sigma(T2B) + \sigma(B2T) + \sigma(L2R) + \sigma(R2L)}{4} \quad (4)$$

$$\overline{\sigma} = \frac{\sigma(0^0) + \sigma(90^0) + \sigma(180^0) + \sigma(270^0)}{4} \quad (5)$$

The value of this measure ranges from 0 to 1 and represents the percentage of percolation. We prepared the succolarity map of the area using the minimum of mean succolarity with a moving window of the size of (50″×50″). Like in case of FD and LA plots, SA plot of the 10 selected regions was also prepared using the mean succolarity value. In the same fashion, SA values were alienated into three categories i.e. low (< 0.5), medium (0.5 to 0.75) and high values (> 0.75). The textures exhibiting highly succolarating behaviour represent the remote location of existing material pixels (impenetrable mass) over a filament i.e. the streams are at remote location. In the active tectonics setting, the high SA values represent an increased susceptibility to surface deformation because of the high percentage of vacant gaps and the existence of lengthy filaments. These filaments are caused by the presence of neotectonic lineaments in the regions. The low SA values correspond to the regions where the geological circumstances stopped the growth of lineaments and thus high drainage density dominates there.

3 Results and Discussions

In tectonically active areas drainage systems are often influenced by the type, geometry and the recent activity of the regional and local faults. In Hindukush (NE-Afghanistan), most drainage networks are influenced by the neotectonic processes. Drainage network analysis in the framework of surface deformation is of great significance as they are the recorders of tectonic and erosional processes. These processes change the drainage network from dendritic to linear and sometimes disconnect due to uplift. The drainage network morphology of the Hindukush is evidently influenced by tectonic forcing (Figure 2). The spatially distributed drainage patterns in the Hindukush are of three types, parallel and dendritic and disconnected. These transitions stages and development from one type to the other are highly indebted to spatio-temporal, climatic and geotectonic processes. The highly steep zones give rise to parallel drainage patterns and verify that they are geotectonically controlled. The local uplift conditions also result in the highly steepened regions, causing the drainage network to be linearized which is evidence of uplifted conditions. The disconnected and rugged drainage patterns show that it is part of a complex tectonic setting. The uninterrupted river networks follow basic fractal geometry, and hence they are differentiated using various fractal measures, i.e., FD, LA and SA. The FD enables us to measure the degree of complexity by calculating how a dimension measurement increases or decreases at various scales. The aim is to quantify the influence of neotectonic activity on the drainage network by measuring the reduction of complexity as the deformation intensity increases. This means that for a highly susceptible site, lower fractal dimension values should be obtained. We anticipate that the drainage network slacks its complexity (dendricity) and become linearized as topographical changes triggered by faults modify the flow network geometry. For this purpose we implemented a BCM.

The FD for six rivers in the study area shown in (Figure 5) and are equal to the Euclidian dimension 1. These low FD values in Hindukush signify the existence of controlling processes (erosion and uplift) on the tectonic evolution of the landscape (Guillermo et al. 2004). Low FD also suggests that the drainage network have undergone a change from natural meandering pattern to linearization due to active tectonic deformation processes. The FD distribution map (Figure 5a) was prepared using the BCM, which shows the spatial anomaly in the drainage patterns. This map shows that the most of the Hindukush regions is characterized by low FD values i.e. highly deformed regions. Very low values of FD are observed in the Panjsher, Andarab, Alingar, Qunduz, Sarobi and Konar regions, which are separately known as active regions (Mahmood et al. 2009). High fractal values are only observed near the main channel of the Kabul River near Kabul city and south of the Kabul and near Jalalabad basin. This means that the drainage patterns here are more dendritic and are controlled mostly by erosion processes and thus show low susceptibility. In a relative and comprehensive analysis, the lowest values of FD were identified at ten sites of the study area. These regions are labeled and shown in (Figure 5a) and their fractal values are shown in Table 1.

Table 1 Summary for three fractal measure for 10 test sites

Region #	Fractal dimension (FD)	Maximum lacunarity (LA)	Mean succolarity (SA)
1	1.29	1.61	0.90
2	1.30	1.49	0.88
3	1.28	1.58	0.90
4	1.30	1.49	0.69
5	1.31	1.41	0.80
6	1.30	1.53	0.90
7	1.32	1.45	0.86
8	1.30	1.34	0.82
9	1.34	1.16	0.52
10	1.41	1.23	0.49

All these selected 10 sites have high vulnerability of surface deformation as the FD values are less than or around 1.30. Because of the varied neotectonics environments, these values suggest a likely correlation between the composite scaling properties of the developed drainage network and the vulnerability of active deformation. The drainage patterns of these sites approach linearity by branching out the filling spaces. The

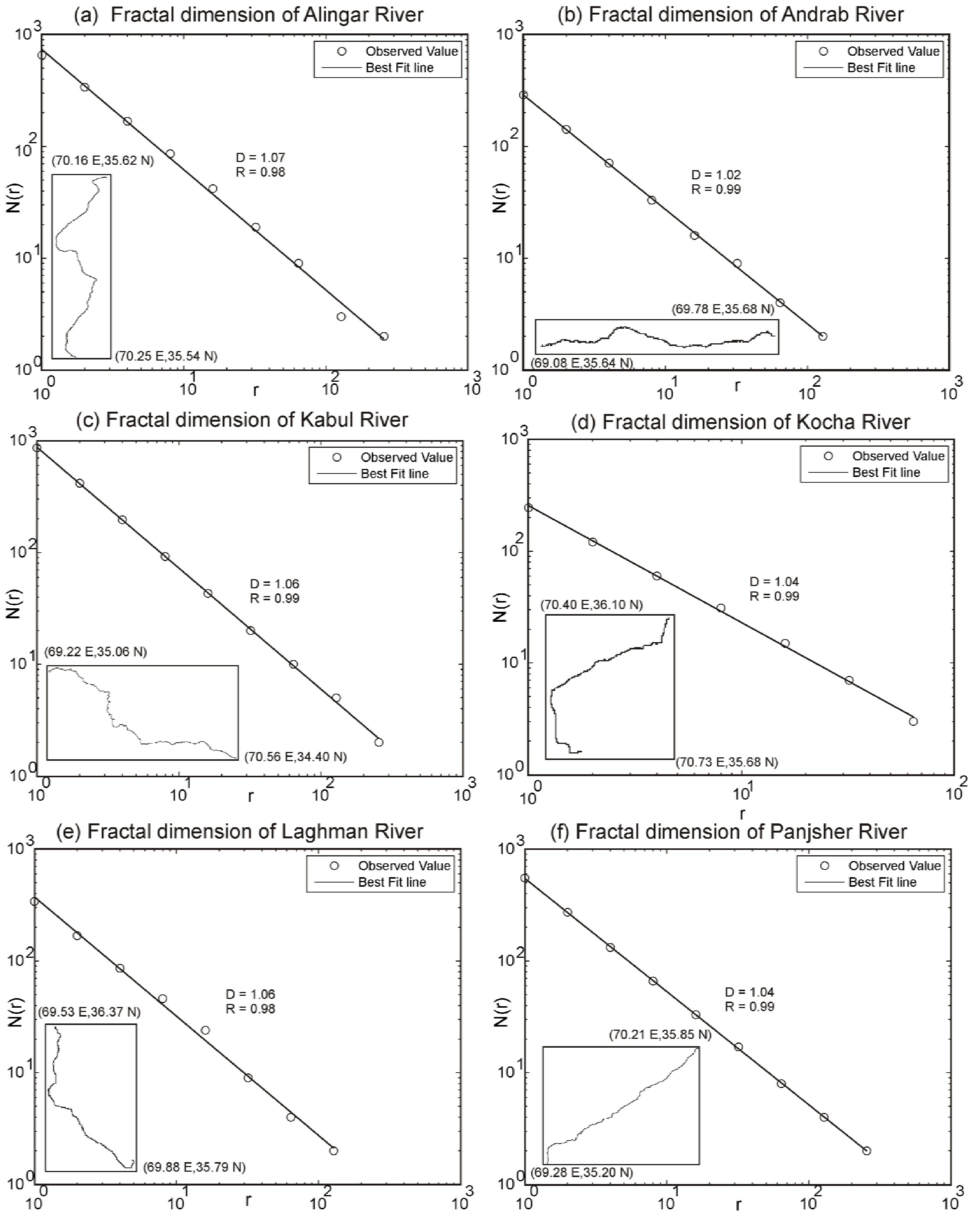

Figure 5 Estimated fractal dimension for Alingar, Andrab, Kabul, Kocha, Laghman and Panjsher Rivers with insets showing their location and nature of orientation

low values of FD of these areas also imply the recent steepening of the landscape. Alongside the 9 just before the Kabul basin, the Alingar River as well as its tributaries is highly linearized. In region 4, the Kocha River takes a sharp turn and changes from direction S-N to NE. This abrupt variation in drainage patterns causes the variety in FD values. In region 3, the Baghlan River becomes linearized before turning towards the south from initial NW direction and produces very low FD values. Though the estimation of the space filling nature of drainage network can disclose the susceptibility to deformation, it is very hard to distinguish between the patterns with diverse vacant gaps dissemination. It simply means that diverse drainage patterns can exhibit same FD values, but their vacant gaps are disseminated differently. Consequently, the regions can be analyzed furtherly based on their deviation from translation invariance. The LA is a perfect tool for the actively deforming regions where it normally shows deviation from translational invariance. High LA means that the image is variant in terms of its vacant gaps dissemination. The drainage patterns are influenced by plentiful mechanisms of gap filling which are reliant upon the active processes in operation. The LA can be used to spot the steep regions that are uplifted and deformed consistently. The high values of LA stand for the regions with high deviation from translation invariance. In general, medium to high lacunarity was observed in the areas with high FD. The drainage deviation from translation invariance of different sites shows that they have been influenced by geological processes at different times. If these areas are under neotectonic influence, then they exhibit comparatively high deviations from the areas that are mainly controlled by erosion processes. The sites with low FD and high LA can not be taken as extremely deformed areas as they ignore the basic assumption of susceptibility to surface deformation based on high FD values. The 10 selected sites having same FD values are then considered for LA analysis (Figure 5b). The LA values for these sites are shown in Table 1. The areas with high FD show medium to high LA values. The sites 1, 6, 8, and 9 can be recognized easily. The low FD values and high relative LA shows that sites 1, 9 and 6 are extremely deformed, while sites 2, 3, 4, 5 and 5 are comparatively less deformed to all 10 sites. The region 6 and 8 are located near the Sarobi fault and the active HF, PSF, GA, KF and SPF (Figure 1, Figure 6) bound this region. These areas are extremely deformed as they have experienced extreme deformation due to continuously ongoing frequent earthquakes in Hindukush. The deflection of rivers and stream channels is further evidence of recent fault activity and this geomorphic evidence indicate that most of these zones have a strike slip sense of movement (Mahmood et al. 2008, 2009).

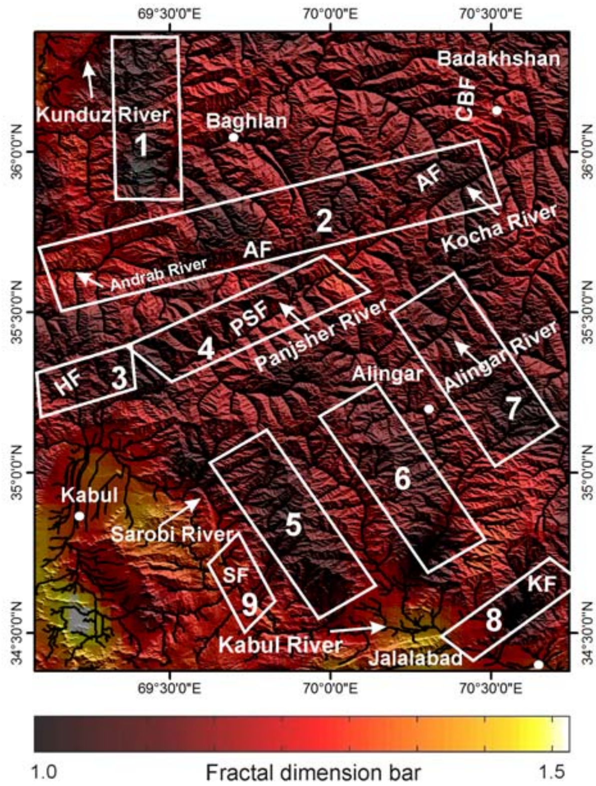

Figure 6 FD distribution map of the study area showing tectonic boundaries. The marked difference between the older northeast-trending structures (blocks, 2, 3, 4 and 8) and the younger north- to northwest-trending features (blocks 1, 5, 6, 7 and 9) suggests that a change in the surface deformational style and mechanics has occurred, from an initial phase of contraction, to a more recent phase of shearing and northwest-directed crustal extrusion along strike-slip fault zones.

Geologically, this is a region of transpression and contains a diverse array of fault types and orientations. The marked difference between the older northeast-trending structures and the younger north- to northwest-trending features suggests that a change in deformational style and mechanics has occurred, from an initial phase of contraction, to a more recent phase of shearing and northwest-directed crustal extrusion along strike-slip fault zones (Figure 2, Figure 6). In the context of India-Eurasia collision, the drainage linearization may be accredited to a two phase deformation of the Himalayan orogeny i.e. first disconnectivity and then forceful steepening. The LA plot (Figure 5d) shows that it is not easy to distinguish between 10 sites because the curves are mingled or intersecting each other. This is why the drainage patterns in these regions exhibit the same gap filling property.

Thus, the SA becomes an inevitable complimentary tool to FD and LA at this important stage of differentiating, when the fractals have the same values. The junction of two or more streams at steep angles is typically ascribed by the localized tectonic control. When the drainage networks exhibit same pattern of occupying gaps and show translation invariance, then SA enables us to compute their orientation and explain the additional categorization. In this investigation, the SA was applied on all 10 sites because at some stage FD and LA can not further distinguish the relative susceptibility to deformation. In this scenario, the texture is not differentiated based on the gap occupation and translation invariance, but on the basis of the drainage pattern orientation. The SA was conducted using the minimum of mean SA values along four likely directions (Figure 5d) explained in the methodology section. The spatial distribution of SA values classifies the study area in two zones i.e. northern, southern zone. These two zones exhibit different structural orientation, hence the extremely low SA values can mark their rough boundaries, because the drainage network orientation suddenly changes along the faults. Recent studies (Mahmood et al. 2009; Ruleman 2005; Wheeler et al. 2005; Harp and Crone 2006) also suggest that a change in deformational style and mechanics has occurred, from an initial phase of contraction, to a more recent phase of shearing and northwest-directed crustal extrusion along strike-slip fault zones (Figure 2, Figure 6). The drain of the drainage capacity of the regions 1, 2, 3, 5, 6, 7 and 8 (Figure 4d) suggest that the relative susceptibility to surface deformation of these regions is descending as follow: 6, 3, 1, 2, 7, 8 and 5 as shown in the Table 1. Regions 1, 2, 3, 5, 6, 7 and 8 lie near, Andarab (AF), Panjsher (PSF), Sarobi (SF) and Konar (KF) faults and are intensely deformed. Because the SA depends on the factor of division or box size k and changes accordingly, the gradually decreasing in SA values show that the percolation of these regions are very high at a low factor of division. The diversity of the drainage network is accredited to the presence of neotectonics in these regions. The major factor causing the drainage linearization is the tectonic while lithological control appeared to be far less dominant. Finally, the 10 regions with high susceptibility for surface deformation are ranked with decreasing susceptibility from 6, 3, 1, 2, 7, 8, 5, 4, 9 and 10. It simply means that relative surface deformation can be forecasted from the three fractal measures of the drainage networks. The FD, LA and SA have the capability of highlighting relatively deformed zones in the context of their steepness, homogeneity and the orientation (Figure 7).

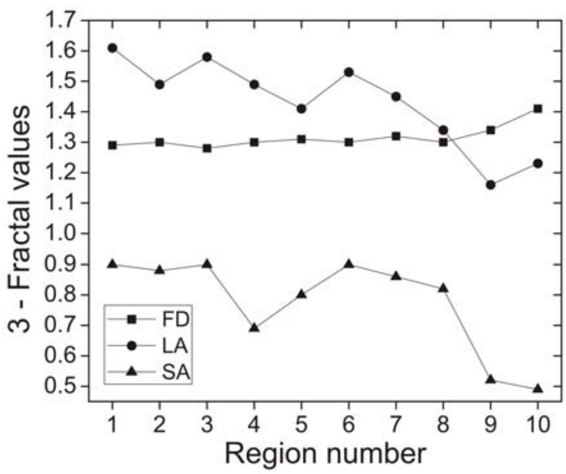

Figure 7 Composite graph showing, FD, LA and SA for the 10 selected test sites. Low FD indicates highly deformed zones, whereas the higher values for LA and SA represent the neotectonic activity for the selected 10 regions.

4 Conclusion

Three fractal analyses are valuable approaches for the quantitative depiction of drainage network evolution and landscape development in the Hindukush. The difference in FD of Kabul, Panjsher, Laghman, Andarab, Alingar and Kocha

Rivers suggests mostly the neotectonic control in the region. The FD map shows the spatial anomaly in the drainage network along 10 identified sites as susceptible to surface deformation. The LA was performed to distinguish further these 10 sites. Even after the LA analysis, the regions still needed the further differentiation for the susceptibility to surface deformation, as the LA curves were intersecting and overlapping. For this reason, we applied SA to differentiate those regions that were not distinguishable even after LA. After SA, it is concluded that the 10 sites in the investigation area possess great susceptibility for surface deformation and these region are ranked with decreasing susceptibility from 6, 3, 1, 2, 7, 8, 5, 4, 9 and 10. The three fractal measures are capable of forecasting the relative dissemination of active deformation. The uplifted regions with variable homogeneity and orientation can be distinguished by three fractal approach. The Hindukush is an active region in the context of India-Eurasia collision zone and has been extremely deformed due to ongoing frequent damaging earthquakes and recent seismicity. This investigation enlightens important socioeconomic aspects by identifying the regions that are highly susceptible to surface deformation. This research can also serve up as a suggestion to the local authorities and Afghan administration for a carefully infrastructure development in deformation prone areas and to take measures for human safety as well.

Acknowledgements

The authors wish to thank University of the Punjab, Lahore-Pakistan, for providing necessary financial assistance to Syed Amer Mahmood to pursue his PHD in Germany. The authors also like to thank the partial support from German Academic Exchange Serivice (DAAD), Germany. The authors also like to thank the anonymous reviewers who gave valuable suggestion that has helped to improve the quality of the manuscript.

References

Allen M, Jackson J, Walker R (2004) Late Cenozoic reorganization of the Arabia-Eurasia collision and the comparison of short-term and long-term deformation rates. Tectonics 23: TC2008, DOI:10.1029/2003TC001530.

Batty M, Longley P (1994) Fractal Cities: A Geometry of Form and Function. London: Academic Press. P 394.

Ben-Zion Y, Sammis CG (2003) Characterization of fault zones. Pure and Applied Geophysics 160: 677-715.

Bull BW (2007). Tectonic Geomorphology of Mountains: A New Approach to Paleoseismology. Blackwell Publishing. p 316.

Dombradi E, Timar G, Gabor B, Sierd C, Frank H (2007). Fractal dimension estimations of drainage network in the Carpathian-Pannonian system. Global and Planetary Change 58(1-4): 197–213.

Dong P (2000). Test of a new lacunarity estimation method for image texture analysis. International Journal of Remote Sensing 21(17): 3369–3377.

Dong P (2009) Lacunarity analysis of raster datasets and 1D, 2D. Computers and Geosciences 35(10): 2100–2110.

Dougherty G, Henebry GM (2001) Fractal signature and lacunarity in the measurement of the texture of trabecular bone in clinical CT images. Medical Engineering & Physics 23(6): 369–380.

Feagina RA, Wub XB, Feaginc T (2007) Edge effects in lacunarity analysis. Ecological Modelling 201(3-4): 262-268.

Foroutan-pour K, Dutilleul P, Smith DL (1999) Advances in the implementation of the box-counting method of fractal dimension estimation. Applied Mathematics and Computation 105(2-3): 195–210.

Gaetani M, Zanchi A, Angiolini L, Olivini G, Sciunnach D, Brunton H, Nicora A, Mawson R (2004) The carboniferous of western Karalorum (Pakistan). Journal of Asian Earth Sciences 23(2): 275–305.

Gardner RH, Hargrove WW, Pretegaard K, Perlmutter M (1996) Lacunarity analysis: A general technique for the analysis of spatial patterns. Physical Review E 53(5): 5461–5468.

Gloaguen R, Marpu PR, Niemeyer I (2007) Automatic extraction of faults and fractal analysis from remote sensing data. Nonlinear Processes in Geophysics 14: 131–138.

Gloaguen R., Kaessner A, Wobbe F, Shahzad F, Mahmood SA (2008) Remote sensing analysis of crustal deformation using river networks. In: IEEE International Geosciences and Remote Sensing Symposium, Boston, USA. pp. IV-1 - IV-4.

Guillermo RA, Gerardo MEP, Piccoloa MC, Pierini J (2004) Fractal analysis of tidal channels in the Bahia Blanca Estuary (Argentina). Geomorphology 57: 263–274.

Harp EL, Crone AJ (2006) Landslides triggered by the October 8, 2005, Pakistan earthquake and associated landslide-dammed reservoirs. In: U.S. Geological Survey Open-File Report 2006–1052. p 10.

Lawrence RD, Khan SH, Tanaka T (1992) Chaman Fault, Pakistan-Afghanistan. In: Buckman RC, Hancock PL. Major Active Faults of the World, Results of the IGCP Project 206. pp 196–223.

Mahmood SA, Shahzad F, Gloaguen R (2008) Remote sensing analysis of quaternary deformation in the Hindukush-pamir region. In: 33rd International Geological Congress, Oslo, Norway.

Mahmood SA, Shahzad F, Gloaguen R (2009) Remote sensing analysis of quaternary deformation using river networks in Hindukush region. In: IEEE International Geosciences and

Remote Sensing Symposium, Cape Town, South Africa. pp II-369 - II-372.
Mandelbrot BB (1983) The Fractal Geometry of Nature. W H Freeman, New York.
Martinez MD, Lana X, Burgueño A, Serra C (2007) Lacunarity, predictability and predictive instability of the daily pluviometric regime in the Iberian Peninsula. Nonlinear Processes in Geophysics 14(2): 109–121.
Marwan N, Saparin P, Kurths J (2007) Measures of complexity for 3D image analysis of trabecular bone. European Physical Journal Special Topics 143: 109–116.
Melo RHC, Conci A (2008) Succolarity: Defining a method to calculate this fractal measure. In: 15th International Conference on Systems, Signals and Image Processing, Bratislava, Slovak Republic. pp 291–294.
Melo RHC, Vieira EA, Conci A (2006) Characterizing the lacunarity of objects and image sets and its use as a technique for the analysis of textural patterns. Lecture Notes in Computer Science 4179: 208–219.
Moreira I. Fractais (1999) In: Nussenzveig H (Org.). Complexidade e caos. Rio de Janeiro: UFRJ/COPEA. pp 51–82. (In Portuguese)
O'Callaghan J, Mark D (1984) The extraction of drainage networks from digital elevation data. Computer Vision Graphics and Image Processing 28(3): 323–344.
Plotnick RE, Gardner RH, O'Neil RV (1993) Lacunarity indices as measures of landscape texture. Landscape Ecology 8(3): 201–211.
Robinson J, Beck R, Gnos E, Vincent RK (2000) New structural and stratigraphic insights for northwestern Pakistan from field and Landsat Thematic Mapper data. GSA Bulletin 112(3): 364–374.
Ruleman CA (2005). Annotated bibliography for Quaternary faulting and geomorphic/tectono-morphic development of Afghanistan. In: Progress Report for Afghan Geologic Hazards Activities: U.S. Geological Survey Internal Report. p 12.
Shahzad F, Mahmood SA, Gloaguen R (2009) Drainage network and lineament analysis: an approach for Potwar Plateau (Northern Pakistan). Journal of Mountain Science 6: 14–24.
Tarboton D, Bras R, Rodriguez-Iturbe I (1991) On the extraction of channel networks from digital elevation data. Hydrological Processes 5: 81–100.
Turcotte DL (1992) Fractals and chaos in geology and geophysics. Cambridge: Cambridge University Press. p 221.
Valous NA, Sun DW, Allen P, Mendoza F (2010). The use of lacunarity for visual texture characterization of pre-sliced cooked pork ham surface intensities. Food Research International 43: 387–395.
Watterson J (1986) Fault dimensions, displacements and growth. Pure and Applied Geophysics 124(1-2): 365–373.
Wheeler RL, Bufe CG, Johnson ML, Dart RL (2005). Seismotectonic map of Afghanistan with annotated bibliography. In: U.S. Geological Survey Open-File Report. p 31.
Wobus CW, Whipple KX, Kirby E, Snyder NP, Johnson J, Spyropolou K, Crosby B, Sheehan DD (2006) Tectonics from topography: Procedures, promise and pitfalls. In: Willett SD, Hovius N, Brandon MT, Fisher DM. Tectonics, Climate and Landscape Evolution. GSA Special Paper 398: 55–74.
Zhang T, Tang G, Liu X, Zhou Y, Jia D (2007) Multi-scale structure of channel network in Jiuyuangou drainage basin. In: Geoinformatics 2007: Geospatial Information Science. p 6753.